

# Experimental characterization of the hierarchy of quantum correlations in top quark pairs

Yoav Afik,<sup>1,\*</sup> Regina Demina,<sup>2,†</sup> Alan Herrera,<sup>2,‡</sup> Otto Heinz  
Hindrichs,<sup>2,§</sup> Juan Ramón Muñoz de Nova,<sup>3,4,¶</sup> and Baptiste Ravina<sup>5,\*\*</sup>

<sup>1</sup>*Enrico Fermi Institute, University of Chicago, Chicago, Illinois 60637, USA*

<sup>2</sup>*Department of Physics and Astronomy, University of Rochester 500 Joseph C. Wilson Boulevard, Rochester, NY 14627, USA*

<sup>3</sup>*Instituto de Estructura de la Materia, IEM-CSIC, Serrano, 123 E-28006 Madrid, Spain*

<sup>4</sup>*Departamento de Física de Materiales, Universidad Complutense de Madrid, E-28040 Madrid, Spain*

<sup>5</sup>*CERN, CH-1211 Geneva, Switzerland*

Recent results from the Large Hadron Collider have demonstrated quantum entanglement of top quark-antiquark pairs using the spin degree of freedom. Based on the doubly differential measurement of the spin density matrix of the top quark and antiquark performed by the CMS collaboration in the helicity and beam bases, we evaluate a set of quantum observables, including discord, steering, Bell correlation, and magic. These observables allow for a quantitative characterization of the quantum correlations present in a top quark-antiquark system, thus enabling an interpretation of collider data in terms of quantum states and their properties. Discord is observed to be greater than zero with a significance of more than  $5\sigma$  standard deviations ( $\sigma$ ). Evidence for steering is found with a significance of more than  $3\sigma$ . This is the first evidence for steering, and the first observation of discord in a high-energy system. No Bell correlation is observed within the currently probed phase space, in agreement with the theoretical prediction. These results experimentally corroborate the full hierarchy of quantum correlations in top quarks with discord being the most basic form of quantum correlation, followed by entanglement, steering and Bell correlation. The significance of nonzero magic, which is a complementary observable to the quantum-correlation hierarchy, is found to exceed  $5\sigma$  in several regions of phase space.

## CONTENTS

I. Introduction	1
II. Theoretical framework	2
A. $t\bar{t}$ system at LHC	2
B. Discord	3
C. EPR paradox, Steering and Bell's theorem	3
D. Magic	3
III. Results	4
IV. Conclusion	7
Acknowledgments	7
References	8
A. More results on discord	10

## I. INTRODUCTION

Quantum mechanics (QM) underpins both quantum information science (QIS) and high-energy physics

(HEP). Despite this shared foundation, the two fields differ significantly in their objectives and have, over time, developed distinct conceptual frameworks and terminologies. While HEP is primarily concerned with understanding the fundamental constituents and forces of nature, QIS is focused on harnessing quantum principles to develop powerful computational and communication technologies. Deepening our understanding of the foundational aspects of QM can lead to further progress in QIS. Although the Large Hadron Collider (LHC) was not originally designed for these studies, it still can serve as a unique laboratory for probing these aspects in a high-energy regime inaccessible elsewhere. To effectively use HEP systems for this purpose, it is important to establish a bridge between QIS and HEP. In this work, based on experimental results, we establish a correspondence between both fields by evaluating a number of fundamental observables common in QIS within a HEP system, in particular top quarks.

Top quark-antiquark pairs ( $t\bar{t}$ ) are produced at the LHC predominantly via gluon-gluon fusion ( $gg$ ), with additional contributions from quark-antiquark annihilation ( $q\bar{q}$ ). Processes involving quark/antiquark-gluon initial states ( $qg$ ) contribute through higher-order QCD corrections. Top quark decays to a  $W$  boson and a  $b$  quark almost 100% of the times [1]. Typically, the  $t\bar{t}$  system is characterized based on the  $W$  bosons decay channels. When both of them decay leptonically, the event is referred to as dilepton. If one  $W$  boson decays to a charged lepton and a neutrino, while the other one decays hadronically to a  $d$ -type ( $d$  or  $s$ ) and a  $u$ -type ( $u$  or  $c$ ) quark, the channel is called lepton+jets, since quarks hadronize

\* [yoavaafik@gmail.com](mailto:yoavaafik@gmail.com)

† [regina@pas.rochester.edu](mailto:regina@pas.rochester.edu)

‡ [alan.herrera@cern.ch](mailto:alan.herrera@cern.ch)

§ [otto.heinz.hindrichs@cern.ch](mailto:otto.heinz.hindrichs@cern.ch)

¶ [jrmnova@fis.ucm.es](mailto:jrmnova@fis.ucm.es)

\*\* [baptiste.ravina@cern.ch](mailto:baptiste.ravina@cern.ch)

into jets.

As the most massive fundamental particle known, with a mass of  $m_t \approx 172.5$  GeV, the top quark has an exceptionally short lifetime ( $\tau_t \approx 5 \times 10^{-25}$  s), which is far shorter than the characteristic timescales for hadronization ( $1/\Lambda_{\text{QCD}} \approx 3 \times 10^{-24}$  s) and spin decorrelation ( $m_t/\Lambda_{\text{QCD}}^2 \approx 2 \times 10^{-21}$  s) [1]. Consequently, the spin information of the top quarks is transmitted directly to their decay products, and their angular distributions can be used to extract the polarizations and spin correlations of a  $t\bar{t}$  pair [2–6].

Based on these properties, various methods were put forward to measure quantum correlations in the  $t\bar{t}$  system, such as discord [7, 8], entanglement [9], steering [7], and Bell correlation [10–16]. Interestingly, these correlations follow a logical hierarchy [17–20], where the presence of Bell correlations implies steerability, which in turn implies entanglement, and this implies discord. Other quantum features, such as magic [21] and contextuality [22], complement the picture provided by this quantum hierarchy. For a non-exhaustive review of the possibility to measure QIS observables in colliders, see Refs. [23, 24].

Entanglement in the  $t\bar{t}$  system was observed by the ATLAS [25] and CMS [26, 27] collaborations at the LHC. These results manifested the entanglement at the highest energy ever probed. Nevertheless, the evaluation of other measures of quantum correlations from the experimental data is still lacking in the literature. Based on the CMS doubly differential measurement of the  $t\bar{t}$  spin density matrix, performed in the lepton+jets channel in the helicity and beam bases at  $\sqrt{s} = 13$  TeV [27, 28], we evaluate quantum discord, steering, Bell correlation, and magic. These quantum observables are evaluated for the first time using LHC data.

## II. THEORETICAL FRAMEWORK

### A. $t\bar{t}$ system at LHC

The top quark has a spin of  $1/2$ , and therefore can be represented as a qubit, the most basic unit of information in QIS. Hence,  $t\bar{t}$  can be represented by a two-qubit system, with its density matrix expanded as

$$\rho_{t\bar{t}} = \frac{1}{4} (I_2 \otimes I_2 + \sum_i P_i \sigma_i \otimes I_2 + \sum_j \bar{P}_j I_2 \otimes \sigma_j + \sum_{ij} C_{ij} \sigma_i \otimes \sigma_j), \quad (1)$$

where  $I_2$  is the  $2 \times 2$  identity matrix,  $\sigma_i$  are Pauli matrices,  $P_i$  and  $\bar{P}_j$  describe the net polarization of the top quark and antiquark, respectively, and  $C_{ij}$  represents their spin correlation matrix. The 3-component vectors  $P_i$ ,  $\bar{P}_j$  and the  $3 \times 3$  matrix  $C_{ij}$  are extracted from the angular correlation of the  $t\bar{t}$  decay products with the highest spin analyzing power ( $\approx 1$ ) – charged leptons and  $d$ -type

quarks [29]. The indices  $i$  and  $j$  correspond to the axes of the basis selected for the measurement.

Common choices for the spin measurement are the beam and helicity bases. Both are right-handed coordinate systems defined in the  $t\bar{t}$  center-of-mass frame [5]. The beam basis is defined by the unit vector  $(\hat{x}, \hat{y}, \hat{z})$ , with the  $x$  axis pointing towards the center of the LHC ring, the  $y$  axis oriented vertically upward, and  $z$  pointing along the proton beam axis,  $\hat{z} = \hat{p}$  [30]. The helicity basis [31] is defined by the unit vectors  $(\hat{k}, \hat{n}, \hat{r})$ , where  $\hat{k}$  denotes the flight direction of the top quark,  $\hat{r} = (\hat{p} - \cos \theta \hat{k}) / \sin \theta$  and  $\hat{n} = \hat{r} \times \hat{k}$ . Here,  $\theta$  is the top quark production angle with respect to  $\hat{p}$ , with  $\cos \theta = \hat{k} \cdot \hat{p}$ . For the helicity basis we use the sign convention of Ref. [6]:

$$\hat{n} \rightarrow \text{sgn}(\cos \theta) \cdot \hat{n}, \quad \hat{r} \rightarrow \text{sgn}(\cos \theta) \cdot \hat{r}, \quad \hat{k} \rightarrow \hat{k}. \quad (2)$$

The evaluation of the different quantum observables considered here depends on the chosen basis. Specifically, in an event-dependent basis, such as the helicity basis, the axis orientation is modified according to the underlying  $t\bar{t}$  kinematics, leading, after integration over some phase-space variables (e.g., an azimuthal angle), to what has been referred to as fictitious quantum states [9, 11, 16, 32]. On the other hand, the beam basis keeps its orientation fixed, leading to *bona fide* quantum states.

In a two-qubit system there are four maximally entangled states, referred to as Bell states:  $|\Phi^\pm\rangle = \frac{1}{\sqrt{2}}(|\uparrow\uparrow\rangle \pm |\downarrow\downarrow\rangle)$  and  $|\Psi^\pm\rangle = \frac{1}{\sqrt{2}}(|\uparrow\downarrow\rangle \pm |\downarrow\uparrow\rangle)$ , where the arrows indicate the spin orientation with respect to the  $\hat{k}$  axis. In Ref. [9] it was predicted that at the threshold of  $t\bar{t}$  production, i.e., when the invariant mass of the  $t\bar{t}$  system,  $m(t\bar{t})$ , is close to twice the mass of the top quark, the system is predominantly in a  $|\Psi^-\rangle$  spin-singlet state. The observed entanglement in the dilepton channel [25, 26] corresponds to this region of the  $t\bar{t}$  phase space. The lepton+jets channel is better suited for the measurements in the higher  $m(t\bar{t})$  region [27, 28], where the system is expected to be predominantly observed in a  $|\Phi^-\rangle$  spin-triplet state [9]. Indeed, in Ref. [28] it was shown that the  $t\bar{t}$  system in the  $m(t\bar{t}) > 800$  GeV,  $|\cos(\theta)| < 0.4$  bin is observed in the  $|\Phi^-\rangle$  state with about 60% fidelity, which is the highest fidelity observed with respect to the Bell basis in the probed phase space. Using the Peres-Horodecki criterion [33, 34], it was demonstrated that the system is in an entangled state in this region of phase space [27].

Here, we use the results of the doubly differential measurement in bins of  $m(t\bar{t})$  vs.  $|\cos(\theta)|$  of the full spin correlation matrix reported in Ref. [27] for the helicity basis and in Ref. [28] for the beam basis. In both cases, we have found a good agreement between the measured spin correlation coefficients and the ones obtained analytically [9, 11].

## B. Discord

In classical information theory, the mutual information of two systems characterizes how much information is obtained about one of them by observing the other. One of the first signatures of QM is the difference between two classically equivalent expressions for the mutual information, quantified by the so-called quantum discord [35]. For a two-qubit  $t\bar{t}$  system, the discord for the top quark reads [36–38]

$$\mathcal{D}_t \equiv S(\rho_{t\bar{t}}) - S(\rho_{t\bar{t}}) + \min_{\hat{u}} \left[ p_{t,+\hat{u}} S(\rho_{t,+\hat{u}}) + p_{t,-\hat{u}} S(\rho_{t,-\hat{u}}) \right], \quad (3)$$

where  $S(\rho) = -\text{Tr}(\rho \log_2 \rho)$  is the von Neumann entropy,  $\rho_t = \text{Tr}_{\bar{t}}[\rho_{t\bar{t}}]$  is the reduced density matrix for the top quark,  $\rho_{\bar{t}} = \text{Tr}_t[\rho_{t\bar{t}}]$  is the reduced density matrix for the top antiquark, and  $\rho_{t,\pm\hat{u}}$  represent the post-measurement quantum states for the top quark given a projective spin-measurement on the top antiquark along a certain quantization axis  $\hat{u}$ , with outcomes characterized by the projectors  $\Pi_{\pm\hat{u}}$ . Specifically,

$$\rho_{t,\pm\hat{u}} = \frac{1}{p_{\pm\hat{u}}} \text{Tr}_t[(I_2 \otimes \Pi_{\pm\hat{u}}) \rho_{t\bar{t}} (I_2 \otimes \Pi_{\pm\hat{u}})], \quad (4)$$

where  $p_{\pm\hat{u}}$  is the probability of each outcome,

$$p_{\pm\hat{u}} = \text{Tr}[(I_2 \otimes \Pi_{\pm\hat{u}}) \rho_{t\bar{t}} (I_2 \otimes \Pi_{\pm\hat{u}})]. \quad (5)$$

Finally, the minimization over the directions of  $\hat{u}$  in Eq. (3) represents the minimization over all possible projective measurements, ensuring the least disturbance on the system by the observation process [35]. In this work, this minimization is performed numerically. A similar expression can be derived for the discord of the top antiquark.

## C. EPR paradox, Steering and Bell's theorem

In their famous 1935 paper, Einstein, Podolsky and Rosen (EPR) questioned the completeness of QM by highlighting a paradox – an apparent incompatibility between quantum predictions and the principles of locality and realism [39]. EPR considered a pair of spatially separated systems prepared in a correlated quantum state, such that the measurement of one system enables a prediction, with certainty, of the outcome of a corresponding measurement on the other. Under the assumption that physical influences cannot propagate superluminally, EPR argued that these correlations imply the existence of elements of reality (hidden variables) not captured by the quantum description, concluding that QM must be incomplete.

The concept of quantum steering, defined as the ability to influence, or “steer”, the quantum state of one system by performing a measurement on another, arises

naturally from the EPR argument. Schrödinger proposed the concept of steering as his interpretation of the EPR paradox [40], but the precise formulation was given much later in Ref. [17]. A two-qubit system in an unpolarized state (i.e.,  $P_i = \bar{P}_j = 0$ ), such as  $t\bar{t}$  at leading-order in QCD [7], is steerable if and only if [41, 42]

$$\mathcal{T} = \int d^2\hat{u} \sqrt{\hat{u}^T C^T C \hat{u}} > 2\pi, \quad (6)$$

where the integral is taken over all possible orientations of the unit vector  $\hat{u}$ .

The formulation of the EPR paradox initiated a sustained experimental and theoretical effort to characterize nonclassical correlations. A Bell inequality sets an upper bound on the correlations between measurement outcomes on two subsystems that must be respected by local hidden-variable theories (LHVTs). Bell's theorem [43] shows that, although all LHVTs satisfy these inequalities, the correlations predicted by QM can violate them. Experimental tests have indeed observed such violations [44–47], thereby ruling out LHVTs and supporting the QM description of nature.

In our case we rely on quantum state tomography of the two-qubit system, used to reconstruct the underlying quantum state. This strategy does not constitute a direct test of Bell inequality and, thus, cannot exclude LHVTs [48–50]. Instead, it assesses whether the reconstructed state would be expected to violate a standard Bell test.

A useful form of Bell inequality is the Clauser-Horne-Shimony-Holt (CHSH) inequality [51], which is violated in a two-qubit system if and only if the two largest eigenvalues of  $C^T C$  ( $m_1$  and  $m_2$ ) satisfy [7, 10, 52]:

$$\mathcal{B} = m_1 + m_2 > 1. \quad (7)$$

A state fulfilling this criterion is referred to as a Bell-correlated state [53]. The experimental observation of such state at the LHC is of great interest [54, 55], since it would demonstrate that the most extreme manifestations of quantum behavior can be also achieved in high-energy colliders.

It is known that quantum correlations follow a well-structured hierarchy [17–20], with discord being the most basic one, followed by entanglement, steering, and then Bell correlation.

## D. Magic

Quantum computers promise significant advantages over classical computation [56]. Key quantum phenomena such as superposition and entanglement enable quantum algorithms to achieve exponential or polynomial speedups for specific classes of problems compared to their classical counterparts [57–60]. However, the Gottesman-Knill theorem [61] states that quantum circuits involving only stabilizer states, defined as the si-

multaneous eigenstates of a set of commuting Pauli operators, and operations from the Clifford group can be efficiently simulated on a classical computer. For example, Shor's algorithm [57], which forms the foundation of quantum cryptographic systems, is based on non-Clifford gates, and offers polynomial-time solutions to integer factorization, a task that is classically considered sub-exponential in complexity. Quantum magic is a property of quantum states that quantifies their potential computational advantage over classical states. Any stabilizer state has zero magic, whereas quantum states with higher magic provide a greater computational advantage over classical systems. Magic is also studied in broader contexts such as black hole dynamics, where the growth of their interiors cannot be explained by entanglement on the boundary alone [62], and in other fields such as quantum chaos, many-body theory, and in potential simulations of quantum gravity [63–72].

A general form of magic  $\tilde{\mathcal{M}}_2$  for mixed quantum states, such as the  $t\bar{t}$  system, is defined based on the second stabilizer Rényi entropy [73, 74] and can be evaluated as:

$$\tilde{\mathcal{M}}_2 = -\log_2 \left( \frac{1 + \sum_i [(P_i^4 + \bar{P}_i^4)] + \sum_{i,j} C_{ij}^4}{1 + \sum_i [(P_i^2 + \bar{P}_i^2)] + \sum_{i,j} C_{ij}^2} \right). \quad (8)$$

### III. RESULTS

We evaluate quantum discord using Eq. (3), steering using Eq. (6), Bell correlations using Eq. (7), and quantum magic using Eq. (8). The optimal values of these observables and the confidence intervals are estimated by minimizing the negative logarithm of the likelihood function ( $L$ ) defined by

$$-2 \log(L) = \sum_{i,j} (o_i - x_i) U_{ij}^{-1} (o_j - x_j), \quad (9)$$

where  $o_i$  are the observed values of the polarization and spin correlation coefficients in a given  $m(t\bar{t})$  vs.  $|\cos(\theta)|$  bin with the covariance matrix  $U_{ij}$ , and  $x_i$  are the corresponding parameters of the likelihood, constrained to be within the physically allowed region  $-1 \leq x_i \leq 1$  (in practice, these limits are never reached). The central value for each observable, i.e.  $\mathcal{D}_t$ ,  $\mathcal{T}$ ,  $\mathcal{B}$  or  $\tilde{\mathcal{M}}_2$ , is determined by  $-2 \log(L) = 0$ . We scan the range around this central value and, while keeping the value of the observable constant, we minimize the expression in Eq. (9) by varying  $x_i$ . The 68% confidence interval is defined by  $-2 \log(L) = 1$ . If this value is not reached for the physically allowed range of the observable, we quote the distance from the boundary, i.e., zero. Whenever applicable, we also determine the exclusion limits for the threshold conditions, i.e., zero for discord and magic,  $2\pi$  for steering, and one for Bell correlation. The results for all observables are presented in Tabs. I and II for the helicity and beam bases, respectively.

The results are compared to the values predicted by the Standard Model (SM) using the Monte Carlo simulated samples described in Refs. [27, 28]. Since the predictions from the different Monte Carlo simulations employed in these analyses show a good agreement with each other, we include only the one obtained with the POWHEG v2 [75–77] matrix-element generator with PYTHIA 8.2 [78] used for the parton-shower simulation.

The measurement of the quantum discord of the top quark in the helicity and beam bases in bins of  $m(t\bar{t})$  vs.  $|\cos(\theta)|$  is presented in Fig. 1 (upper row). In the helicity basis, the highest value of discord is observed in the high  $m(t\bar{t})$  and low  $|\cos(\theta)|$  region, where it exceeds zero with greater than  $5\sigma$  significance. Notably, this region also coincides with the strongest entanglement significance reported in Ref. [27]. In addition, in several bins we find nonzero discord with  $> 5\sigma$  significance as shown in Tabs. I and II, despite the system being in a separable state ( $\Delta_E \leq 1$ ), which demonstrates the presence of quantum correlations in  $t\bar{t}$  production that are not captured by entanglement. In the beam basis, the highest value of discord is obtained in the region with low  $m(t\bar{t})$  and high  $|\cos(\theta)|$ . It is also important to note that in the high  $m(t\bar{t})$  region discord approaches zero, meaning that the beam basis is not optimal for observing the quantum nature of correlations outside the threshold region.

The definition of discord is not necessarily symmetric under exchanging the top quark and antiquark. For completeness, we present the quantum discord of the top antiquark ( $\mathcal{D}_{\bar{t}}$ ) in App. A. As discussed in Ref. [7], the deviation from zero in the difference between the discord of the top quark and antiquark would signal the presence of  $CP$ -violating physics beyond the SM. We therefore also include in App. A the difference  $\mathcal{D}_t - \mathcal{D}_{\bar{t}}$ , which we find to be consistent with the SM expectation of zero.

The steering results for helicity and beam bases in bins of  $m(t\bar{t})$  vs.  $|\cos(\theta)|$  are presented in Fig. 1 (middle row). In the helicity basis, we observe the highest and the most significant value of steering in the  $m(t\bar{t}) > 800$  GeV,  $|\cos(\theta)| < 0.4$  bin. The observed value of  $8.55^{+0.65}_{-0.65}$  exceeds the threshold value of  $2\pi$  by more than  $3\sigma$ , presenting the first evidence for steerability in the  $t\bar{t}$  system. This indicates that, in the phase space region where entanglement has been observed [27], the quantum correlations in the system are strong enough to even exhibit evidence for steerability.

The Bell correlations for helicity and beam bases in bins of  $m(t\bar{t})$  vs.  $|\cos(\theta)|$  are presented in Fig. 1 (bottom row). The highest value of  $\mathcal{B} = 0.99^{+0.20}_{-0.17}$  is observed in the helicity basis in the  $m(t\bar{t}) > 800$  GeV,  $|\cos(\theta)| < 0.4$  bin, which does not quite reach the threshold value of 1.

In Fig. 2 the extracted values of magic are shown in bins of  $m(t\bar{t})$  vs.  $|\cos(\theta)|$  for the helicity and beam bases, demonstrating a good agreement with the SM predictions. In the helicity basis the highest  $\tilde{\mathcal{M}}_2$  value is observed for low  $m(t\bar{t})$ , however, the most significant result is found at high  $m(t\bar{t})$  and low  $|\cos(\theta)|$ . In the beam basis we observe the highest  $\tilde{\mathcal{M}}_2$  value at low  $m(t\bar{t})$  and high

TABLE I. QIS observables in helicity basis with their uncertainties, determined by  $-2 \log(L) = 1$ . Significance in units of  $\sigma$  above 3.0 of the deviation from the null hypothesis, i.e.,  $\mathcal{D}_t = 0$ ,  $\Delta_E = 1$ ,  $\mathcal{T} = 2\pi$ ,  $\mathcal{B} = 1$ ,  $\tilde{\mathcal{M}}_2 = 0$ , is shown in square brackets. Bins where the  $t\bar{t}$  system is in an entangled state are highlighted in bold.

$m(t\bar{t})$ [GeV]	$ \cos(\theta) $	$\mathcal{D}_t$	$\Delta_E$	$\mathcal{T}$	$\mathcal{B}$	$\tilde{\mathcal{M}}_2$
[300, 400]	[0.0, 0.4]	$0.147^{+0.066}_{-0.121}$	$0.71^{+0.25}_{-0.25}$	$4.35^{+0.93}_{-1.19}$	$0.51^{+0.25}_{-0.18}$	$0.47^{+0.15}_{-0.11}[4.6\sigma]$
	[0.4, 0.7]	$0.16^{+0.16}_{-0.11}$	$1.37^{+0.37}_{-0.38}$	$6.2^{+1.3}_{-1.4}$	$0.85^{+0.27}_{-0.24}$	$0.61^{+0.17}_{-0.22}[4.4\sigma]$
	[0.7, 1.0]	$0.18^{+0.11}_{-0.11}[3.4\sigma]$	$1.43^{+0.26}_{-0.26}$	$6.38^{+0.98}_{-0.92}$	$0.80^{+0.17}_{-0.18}$	$0.580^{+0.093}_{-0.133}[4.8\sigma]$
[400, 600]	[0.0, 0.4]	$0.218^{+0.080}_{-0.052}[>5\sigma]$	$0.419^{+0.063}_{-0.064}$	$3.88^{+0.28}_{-0.27}$	$0.240^{+0.037}_{-0.031}$	$0.340^{+0.037}_{-0.035}[>5\sigma]$
	[0.4, 0.7]	$0.111^{+0.042}_{-0.034}[>5\sigma]$	$0.340^{+0.076}_{-0.077}$	$3.12^{+0.33}_{-0.33}$	$0.147^{+0.038}_{-0.032}$	$0.236^{+0.045}_{-0.042}[>5\sigma]$
	[0.7, 1.0]	$0.052^{+0.013}_{-0.011}[>5\sigma]$	$0.945^{+0.061}_{-0.063}$	$4.34^{+0.26}_{-0.25}$	$0.386^{+0.050}_{-0.046}$	$0.394^{+0.027}_{-0.028}[>5\sigma]$
[600, 800]	[0.0, 0.4]	$0.107^{+0.056}_{-0.032}[>5\sigma]$	$1.029^{+0.098}_{-0.096}$	$4.85^{+0.36}_{-0.36}$	$0.490^{+0.073}_{-0.069}$	$0.431^{+0.041}_{-0.037}[>5\sigma]$
	[0.4, 0.7]	$0.091^{+0.044}_{-0.030}[>5\sigma]$	$0.58^{+0.11}_{-0.11}$	$3.19^{+0.25}_{-0.36}$	$0.210^{+0.048}_{-0.044}$	$0.260^{+0.050}_{-0.048}[>5\sigma]$
	[0.7, 1.0]	$0.033^{+0.015}_{-0.012}[3.6\sigma]$	$0.475^{+0.087}_{-0.089}$	$2.21^{+0.39}_{-0.40}$	$0.121^{+0.042}_{-0.034}$	$0.163^{+0.050}_{-0.044}[>5\sigma]$
[800, 13000]	[0.0, 0.4]	$0.424^{+0.078}_{-0.091}[>5\sigma]$	$2.03^{+0.15}_{-0.15}[>5\sigma]$	$8.55^{+0.65}_{-0.65}[3.6\sigma]$	$0.99^{+0.20}_{-0.17}$	$0.561^{+0.042}_{-0.066}[>5\sigma]$
	[0.4, 0.7]	$0.158^{+0.046}_{-0.070}[>5\sigma]$	$1.15^{+0.13}_{-0.13}$	$5.27^{+0.51}_{-0.52}$	$0.617^{+0.100}_{-0.109}$	$0.567^{+0.040}_{-0.056}[>5\sigma]$
	[0.7, 1.0]	$0.033^{+0.019}_{-0.015}[3.1\sigma]$	$0.169^{+0.087}_{-0.088}$	$2.01^{+0.40}_{-0.40}$	$0.071^{+0.035}_{-0.027}$	$0.113^{+0.043}_{-0.037}[5.0\sigma]$

TABLE II. QIS observables in beam basis with their uncertainties, determined by  $-2 \log(L) = 1$ . If this value is not reached for the physically allowed range of the observable, we quote the distance from the boundary, i.e. zero. Significance in units of  $\sigma$  above 3.0 of the deviation from the null hypothesis, i.e.,  $\mathcal{D}_t = 0$ ,  $\Delta_E = 1$ ,  $\mathcal{T} = 2\pi$ ,  $\mathcal{B} = 1$ ,  $\tilde{\mathcal{M}}_2 = 0$ , is shown in square brackets.

$m(t\bar{t})$ [GeV]	$ \cos(\theta) $	$\mathcal{D}_t$	$\Delta_E$	$\mathcal{T}$	$\mathcal{B}$	$\tilde{\mathcal{M}}_2$
[300, 400]	[0.0, 0.4]	$0.187^{+0.132}_{-0.078}[>5\sigma]$	$0.96^{+0.23}_{-0.23}$	$4.51^{+0.79}_{-0.77}$	$0.41^{+0.15}_{-0.13}$	$0.383^{+0.063}_{-0.078}[>5\sigma]$
	[0.4, 0.7]	$0.177^{+0.143}_{-0.084}[3.4\sigma]$	$1.26^{+0.41}_{-0.41}$	$5.3^{+1.7}_{-1.6}$	$0.44^{+0.29}_{-0.21}$	$0.48^{+0.10}_{-0.17}[3.5\sigma]$
	[0.7, 1.0]	$0.376^{+0.127}_{-0.083}[>5\sigma]$	$1.88^{+0.28}_{-0.28}[3.2\sigma]$	$7.9^{+1.1}_{-1.1}$	$0.94^{+0.23}_{-0.21}$	$0.543^{+0.039}_{-0.085}[4.6\sigma]$
[400, 600]	[0.0, 0.4]	$0.209^{+0.035}_{-0.026}[>5\sigma]$	$0.360^{+0.036}_{-0.034}$	$3.93^{+0.22}_{-0.22}$	$0.211^{+0.029}_{-0.026}$	$0.329^{+0.027}_{-0.027}[>5\sigma]$
	[0.4, 0.7]	$0.127^{+0.031}_{-0.027}[>5\sigma]$	$0.452^{+0.067}_{-0.066}$	$3.30^{+0.26}_{-0.27}$	$0.186^{+0.032}_{-0.030}$	$0.251^{+0.033}_{-0.032}[>5\sigma]$
	[0.7, 1.0]	$0.1101^{+0.0092}_{-0.0137}[>5\sigma]$	$1.004^{+0.059}_{-0.059}$	$4.21^{+0.25}_{-0.25}$	$0.237^{+0.037}_{-0.033}$	$0.365^{+0.030}_{-0.031}[>5\sigma]$
[600, 800]	[0.0, 0.4]	$0.017^{+0.019}_{-0.012}$	$0.545^{+0.052}_{-0.053}$	$3.58^{+0.35}_{-0.34}$	$0.301^{+0.060}_{-0.055}$	$0.264^{+0.019}_{-0.024}[>5\sigma]$
	[0.4, 0.7]	$0.0132^{+0.0160}_{-0.0095}$	$0.351^{+0.056}_{-0.055}$	$2.45^{+0.37}_{-0.37}$	$0.131^{+0.042}_{-0.037}$	$0.162^{+0.038}_{-0.038}[>5\sigma]$
	[0.7, 1.0]	$0.034^{+0.012}_{-0.0101}[4.9\sigma]$	$0.503^{+0.079}_{-0.078}$	$2.12^{+0.32}_{-0.33}$	$0.064^{+0.022}_{-0.020}$	$0.114^{+0.035}_{-0.030}[>5\sigma]$
[800, 13000]	[0.0, 0.4]	$0.003^{+0.034}_{-0.003}$	$0.721^{+0.083}_{-0.082}$	$4.56^{+0.53}_{-0.53}$	$0.52^{+0.13}_{-0.11}$	$0.260^{+0.019}_{-0.043}[3.4\sigma]$
	[0.4, 0.7]	$0.0004^{+0.0093}_{-0.0004}$	$0.609^{+0.067}_{-0.069}$	$3.82^{+0.43}_{-0.42}$	$0.370^{+0.087}_{-0.078}$	$0.2686^{+0.0074}_{-0.0172}[>5\sigma]$
	[0.7, 1.0]	$0.0013^{+0.0035}_{-0.0013}$	$0.181^{+0.078}_{-0.078}$	$0.86^{+0.34}_{-0.33}$	$0.0153^{+0.0154}_{-0.0096}$	$0.023^{+0.021}_{-0.014}$

$|\cos(\theta)|$ .

To illustrate the hierarchy of the quantum correlations, we select three bins and plot the significance of the discord, entanglement (from Refs. [27, 28]), steering and Bell correlation markers exceeding the respective threshold values in Fig. 3. In the first bin, the hierarchy of the quantum observables is most apparent. The second bin exemplifies the case where a significant value of discord is observed despite  $t\bar{t}$  being in a separable state. In the third bin,  $t\bar{t}$  is observed in an entangled state, the significance of discord exceeds  $5\sigma$ , while the significance of steering is above  $3\sigma$ . Bell correlation is not observed in this, or any other bin probed in this study. In Ref. [12] it was argued that Bell correlation might be observed in the  $t\bar{t}$  system in the region of phase space with even higher  $m(t\bar{t})$  and lower  $|\cos(\theta)|$ . To have sufficient statistics to

measure spin correlations in this region of phase space, a larger  $t\bar{t}$  sample must be collected.

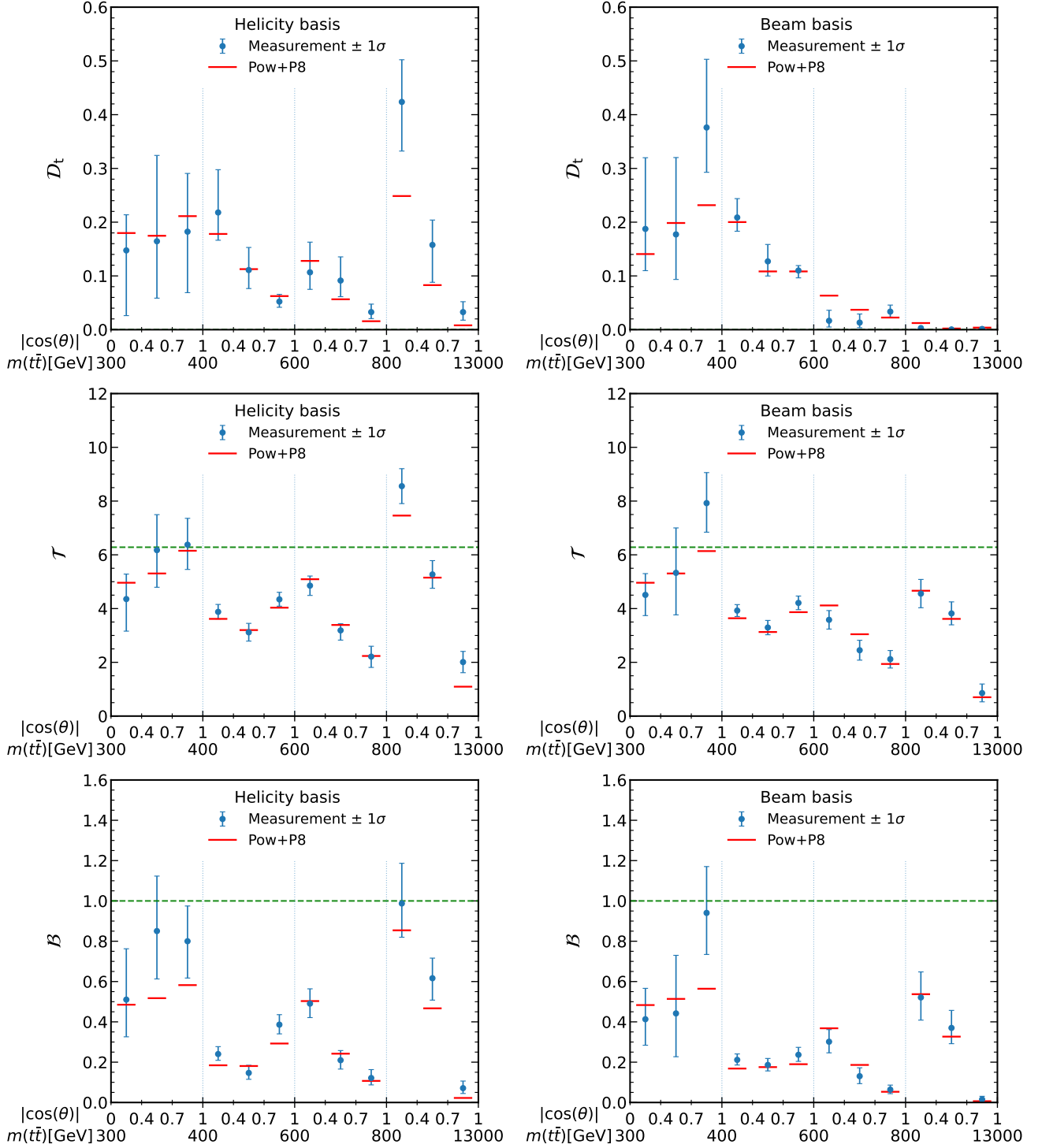


FIG. 1. Results for quantum discord  $D_t$  (upper row), steering marker  $\mathcal{T}$  (middle row), and Bell correlation marker  $\mathcal{B}$  (bottom row) in bins of  $m(t\bar{t})$  vs.  $|\cos(\theta)|$  in the helicity (left) and beam (right) bases. The measurements (points) are shown with the total uncertainty and compared to the predictions of POWHEG+PYTHIA. Horizontal dashed lines indicate the threshold values:  $2\pi$  for  $\mathcal{T}$ , one for  $\mathcal{B}$ . The threshold value for  $D_t$  is zero.

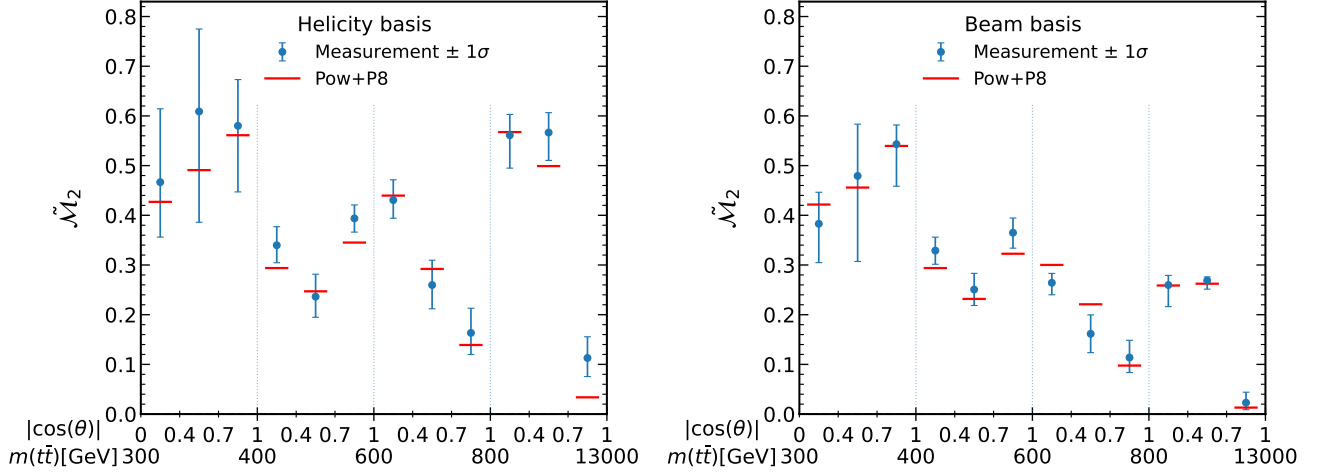


FIG. 2. Quantum magic  $\tilde{\mathcal{M}}_2$  in the helicity (left) and beam (right) bases in bins of  $m(t\bar{t})$  vs.  $|\cos(\theta)|$ . The measurements (points) are shown with the total uncertainty and compared to the predictions of POWHEG+PYTHIA. The threshold value for  $\tilde{\mathcal{M}}_2$  is zero.

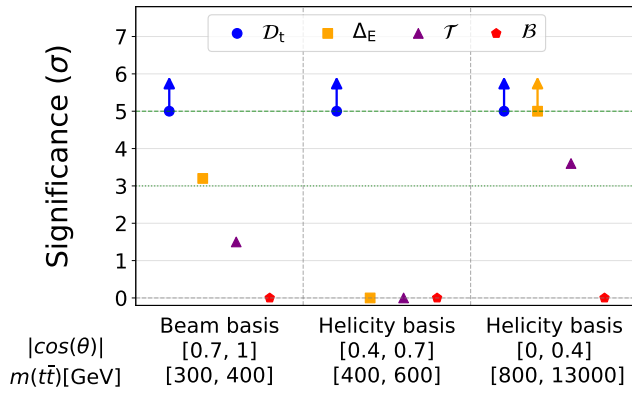


FIG. 3. Significance in units of  $\sigma$  of the discord, entanglement, steering and Bell correlation markers exceeding the threshold values.

#### IV. CONCLUSION

Production of top quark-antiquark pairs at the LHC offers a unique opportunity to study the fundamental aspects of quantum mechanics in the high-energy regime. In this paper, we present the first evaluation of a number of quantum information properties, specifically discord, steering, Bell correlation, and magic, of the top quark-antiquark system. The observables are derived from the doubly differential measurements of top quark polarization and spin correlation coefficients published by the CMS collaboration, performed in the helicity and beam bases, where the former basis characterizes fictitious quantum states due to its event-dependent spatial orientation, while the latter leads to *bona fide* spin quantum states as its orientation is fixed. We observe that discord, which constitutes the most basic form of quan-

tum correlations, is greater than zero with a significance of more than  $5\sigma$  in several regions of phase space, some of which correspond to a separable quantum state. This observation demonstrates that entanglement is not a necessary condition for a quantum behavior of the  $t\bar{t}$  system. We also find that the proposed steering marker exceeds the threshold value with a significance greater than  $3\sigma$ . The threshold value for Bell correlation is not reached. Bell correlations are not expected to arise within the regions of phase space probed in this study, but instead in the regions beyond the reach of the currently available datasets.

Notably, the statistical significance of each observable reflects its position in the hierarchy of quantum correlations: tighter correlations are significant only within a smaller region of phase space and therefore, within a given bin, they exhibit lower statistical significance as they are more difficult to observe. Magic, which quantifies a potential advantage for quantum computation and is a complementary observable to the quantum-correlation hierarchy, is found to be greater than zero with a significance of more than  $5\sigma$  in several regions of phase space.

Future measurements, incorporating the larger datasets anticipated from Run 3 of the LHC, are expected to improve the sensitivity to Bell correlations and quantum steering. Finally, several studies have shown that quantum correlations constitute a sensitive tool for probing physics beyond the SM [79–83], and the results presented in this work may contribute to such investigations.

#### ACKNOWLEDGMENTS

AH, OH and RD acknowledge support from the U.S.

Department of Energy under the grant DE-SC0008475. YA is supported by the National Science Foundation under Grant No. PHY-2310094. JRMDN acknowledges funding from European Union's Horizon 2020 research and innovation programme under the

Marie Skłodowska-Curie Grant Agreement No. 847635, and from Spain's MICIU/AEI through Proyectos de Generación de Conocimiento (Grant No. PID2022-139288NB-I00) and through Ramón y Cajal program (Grant No. RYC2024-050437-I).

---

[1] S. Navas *et al.* (Particle Data Group), Review of particle physics, *Phys. Rev. D* **110**, 030001 (2024).

[2] W. Bernreuther and A. Brandenburg, Tracing CP violation in the production of top quark pairs by multiple TeV proton proton collisions, *Phys. Rev. D* **49**, 4481 (1994), [arXiv:hep-ph/9312210](https://arxiv.org/abs/hep-ph/9312210).

[3] W. Bernreuther, M. Flesch, and P. Haberl, Signatures of Higgs bosons in the top quark decay channel at hadron colliders, *Phys. Rev. D* **58**, 114031 (1998), [arXiv:hep-ph/9709284](https://arxiv.org/abs/hep-ph/9709284).

[4] W. Bernreuther, A. Brandenburg, Z. G. Si, and P. Uwer, Top-quark spin correlations at hadron colliders: Predictions at next-to-leading order qcd, *Phys. Rev. Lett.* **87**, 242002 (2001).

[5] W. Bernreuther, A. Brandenburg, Z. G. Si, and P. Uwer, Top quark pair production and decay at hadron colliders, *Nucl. Phys. B* **690**, 81 (2004), [arXiv:hep-ph/0403035](https://arxiv.org/abs/hep-ph/0403035).

[6] W. Bernreuther, D. Heisler, and Z.-G. Si, A set of top quark spin correlation and polarization observables for the lhc: Standard model predictions and new physics contributions, *Journal of High Energy Physics* **2015**, 1 (2015).

[7] Y. Afik and J. R. Muñoz de Nova, Quantum Discord and Steering in Top Quarks at the LHC, *Phys. Rev. Lett.* **130**, 221801 (2023), [arXiv:2209.03969](https://arxiv.org/abs/2209.03969) [quant-ph].

[8] T. Han, M. Low, N. McGinnis, and S. Su, Measuring quantum discord at the LHC, *JHEP* **05**, 081, [arXiv:2412.21158](https://arxiv.org/abs/2412.21158) [hep-ph].

[9] Y. Afik and J. R. Muñoz de Nova, Entanglement and quantum tomography with top quarks at the LHC, *Eur. Phys. J. Plus* **136**, 907 (2021), [arXiv:2003.02280](https://arxiv.org/abs/2003.02280) [quant-ph].

[10] M. Fabbrichesi, R. Floreanini, and G. Panizzo, Testing Bell Inequalities at the LHC with Top-Quark Pairs, *Phys. Rev. Lett.* **127**, 161801 (2021), [arXiv:2102.11883](https://arxiv.org/abs/2102.11883) [hep-ph].

[11] Y. Afik and J. R. Muñoz de Nova, Quantum information with top quarks in QCD, *Quantum* **6**, 820 (2022), [arXiv:2203.05582](https://arxiv.org/abs/2203.05582) [quant-ph].

[12] C. Severi, C. D. E. Boschi, F. Maltoni, and M. Sioli, Quantum tops at the LHC: from entanglement to Bell inequalities, *Eur. Phys. J. C* **82**, 285 (2022), [arXiv:2110.10112](https://arxiv.org/abs/2110.10112) [hep-ph].

[13] J. A. Aguilar-Saavedra and J. A. Casas, Improved tests of entanglement and Bell inequalities with LHC tops, *Eur. Phys. J. C* **82**, 666 (2022), [arXiv:2205.00542](https://arxiv.org/abs/2205.00542) [hep-ph].

[14] Z. Dong, D. Gonçalves, K. Kong, and A. Navarro, Entanglement and Bell inequalities with boosted  $t\bar{t}$ , *Phys. Rev. D* **109**, 115023 (2024), [arXiv:2305.07075](https://arxiv.org/abs/2305.07075) [hep-ph].

[15] T. Han, M. Low, and T. A. Wu, Quantum entanglement and Bell inequality violation in semi-leptonic top decays, *JHEP* **07**, 192, [arXiv:2310.17696](https://arxiv.org/abs/2310.17696) [hep-ph].

[16] K. Cheng, T. Han, and M. Low, Optimizing entanglement and Bell inequality violation in top antitop events, *Phys. Rev. D* **111**, 033004 (2025), [arXiv:2407.01672](https://arxiv.org/abs/2407.01672) [hep-ph].

[17] H. M. Wiseman, S. J. Jones, and A. C. Doherty, Steering, entanglement, nonlocality, and the einstein-podolsky-rosen paradox, *Phys. Rev. Lett.* **98**, 140402 (2007).

[18] H. S. Qureshi, S. Ullah, and F. Ghafoor, Hierarchy of quantum correlations using a linear beam splitter, *Scientific reports* **8**, 16288 (2018).

[19] T. J. Baker and H. M. Wiseman, Necessary conditions for steerability of two qubits from consideration of local operations, *Phys. Rev. A* **101**, 022326 (2020).

[20] R. Uola, A. C. S. Costa, H. C. Nguyen, and O. Gühne, Quantum steering, *Rev. Mod. Phys.* **92**, 015001 (2020).

[21] C. D. White and M. J. White, Magic states of top quarks, *Phys. Rev. D* **110**, 116016 (2024), [arXiv:2406.07321](https://arxiv.org/abs/2406.07321) [hep-ph].

[22] M. Fabbrichesi, R. Floreanini, E. Gabrielli, and L. Marzola, Tests of quantum contextuality in particle physics, *Phys. Rev. D* **112**, 033005 (2025), [arXiv:2504.12382](https://arxiv.org/abs/2504.12382) [hep-ph].

[23] A. J. Barr, M. Fabbrichesi, R. Floreanini, E. Gabrielli, and L. Marzola, Quantum entanglement and Bell inequality violation at colliders, *Prog. Part. Nucl. Phys.* **139**, 104134 (2024), [arXiv:2402.07972](https://arxiv.org/abs/2402.07972) [hep-ph].

[24] Y. Afik *et al.*, Quantum information meets high-energy physics: input to the update of the European strategy for particle physics, *Eur. Phys. J. Plus* **140**, 855 (2025), [arXiv:2504.00086](https://arxiv.org/abs/2504.00086) [hep-ph].

[25] G. Aad *et al.* (ATLAS), Observation of quantum entanglement with top quarks at the ATLAS detector, *Nature* **633**, 542 (2024), [arXiv:2311.07288](https://arxiv.org/abs/2311.07288) [hep-ex].

[26] A. Hayrapetyan *et al.* (CMS), Observation of quantum entanglement in top quark pair production in proton–proton collisions at  $\sqrt{s} = 13$  TeV, *Rept. Prog. Phys.* **87**, 117801 (2024), [arXiv:2406.03976](https://arxiv.org/abs/2406.03976) [hep-ex].

[27] A. Hayrapetyan *et al.* (CMS), Measurements of polarization and spin correlation and observation of entanglement in top quark pairs using lepton+jets events from proton–proton collisions at  $\sqrt{s} = 13$  TeV, *Phys. Rev. D* **110**, 112016 (2024), [arXiv:2409.11067](https://arxiv.org/abs/2409.11067) [hep-ex].

[28] A. Hayrapetyan *et al.* (CMS), Characterization of the quantum state of top quark pairs produced in proton–proton collisions at  $\sqrt{s} = 13$  TeV using the beam and helicity bases, Submitted to: Physical Review D Letter (2025), [arXiv:2512.17557](https://arxiv.org/abs/2512.17557) [hep-ex].

[29] A. Brandenburg, Z. G. Si, and P. Uwer, QCD corrected spin analyzing power of jets in decays of polarized top quarks, *Phys. Lett. B* **539**, 235 (2002), [arXiv:hep-ph/0205023](https://arxiv.org/abs/hep-ph/0205023).

[30] S. Chatrchyan *et al.* (CMS), The CMS Experiment at the CERN LHC, *JINST* **3** (2008), S08004.

[31] M. Baumgart and B. Tweedie, A New Twist on Top Quark Spin Correlations, *JHEP* **03** (2013), 117, [arXiv:1212.4888](https://arxiv.org/abs/1212.4888) [hep-ph].

[32] K. Cheng, T. Han, and M. Low, Optimizing fictitious states for Bell inequality violation in bipartite qubit systems with applications to the  $t\bar{t}$  system, *Phys. Rev. D* **109**, 116005 (2024), arXiv:2311.09166 [hep-ph].

[33] A. Peres, Separability criterion for density matrices, *Phys. Rev. Lett.* **77**, 1413 (1996), arXiv:quant-ph/9604005.

[34] P. Horodecki, Separability criterion and inseparable mixed states with positive partial transposition, *Phys. Lett. A* **232**, 333 (1997), arXiv:quant-ph/9703004.

[35] H. Ollivier and W. H. Zurek, Quantum discord: A measure of the quantumness of correlations, *Phys. Rev. Lett.* **88**, 017901 (2001).

[36] S. Hamieh, R. Kobes, and H. Zaraket, Positive-operator-valued measure optimization of classical correlations, *Phys. Rev. A* **70**, 052325 (2004).

[37] X.-M. Lu, J. Ma, Z. Xi, and X. Wang, Optimal measurements to access classical correlations of two-qubit states, *Phys. Rev. A* **83**, 012327 (2011).

[38] D. Girolami and G. Adesso, Quantum discord for general two-qubit states: Analytical progress, *Phys. Rev. A* **83**, 052108 (2011).

[39] A. Einstein, B. Podolsky, and N. Rosen, Can quantum-mechanical description of physical reality be considered complete?, *Phys. Rev.* **47**, 777 (1935).

[40] E. Schrödinger, Discussion of Probability Relations between Separated Systems, *Mathematical Proceedings of the Cambridge Philosophical Society* **31**, 555 (1935).

[41] S. Jevtic, M. J. W. Hall, M. R. Anderson, M. Zwierz, and H. M. Wiseman, Einstein–Podolsky–Rosen steering and the steering ellipsoid, *J. Opt. Soc. Am. B* **32**, A40 (2015), arXiv:1411.1517 [quant-ph].

[42] H. C. Nguyen and T. Vu, Necessary and sufficient condition for steerability of two-qubit states by the geometry of steering outcomes, *Europhysics Letters* **115**, 10003 (2016).

[43] J. S. Bell, On the Einstein–Podolsky–Rosen paradox, *Physics Physique Fizika* **1**, 195 (1964).

[44] A. Aspect, P. Grangier, and G. Roger, Experimental Realization of Einstein–Podolsky–Rosen–Bohm Gedanken-experiment: A New Violation of Bell’s Inequalities, *Phys. Rev. Lett.* **49**, 91 (1982).

[45] E. Hagley, X. Maître, G. Nogues, C. Wunderlich, M. Brune, J. M. Raimond, and S. Haroche, Generation of Einstein–Podolsky–Rosen Pairs of Atoms, *Phys. Rev. Lett.* **79**, 1 (1997).

[46] A. Go *et al.* (Belle), Measurement of EPR-type flavour entanglement in  $\Upsilon(4S) \rightarrow B^0 \bar{B}^0$  decays, *Phys. Rev. Lett.* **99**, 131802 (2007), arXiv:quant-ph/0702267.

[47] S. Storz *et al.*, Loophole-free Bell inequality violation with superconducting circuits, *Nature* **617**, 265 (2023).

[48] S. A. Abel, H. K. Dreiner, R. Sengupta, and L. Ubaldi, Colliders are Testing neither Locality via Bell’s Inequality nor Entanglement versus Non-Entanglement, arXiv:2507.15949 [hep-ph] (2025).

[49] P. Bechtle, C. Breuning, H. K. Dreiner, and C. Duhr, A critical appraisal of tests of locality and of entanglement versus non-entanglement at colliders, arXiv:2507.15947 [hep-ph] (2025).

[50] S. A. Abel, M. Dittmar, and H. K. Dreiner, Testing locality at colliders via Bell’s inequality?, *Phys. Lett. B* **280**, 304 (1992).

[51] J. F. Clauser, M. A. Horne, A. Shimony, and R. A. Holt, Proposed experiment to test local hidden-variable theories, *Phys. Rev. Lett.* **23**, 880 (1969).

[52] R. Horodecki, P. Horodecki, and M. Horodecki, Violating Bell inequality by mixed spin-1/2 states: necessary and sufficient condition, *Phys. Lett. A* **200**, 340 (1995).

[53] N. Brunner, D. Cavalcanti, S. Pironio, V. Scarani, and S. Wehner, Bell nonlocality, *Rev. Mod. Phys.* **86**, 419 (2014), arXiv:1303.2849 [quant-ph].

[54] M. Low, Addressing local realism through Bell tests at colliders, *Phys. Rev. D* **112**, 096008 (2025), arXiv:2508.10979 [hep-ph].

[55] M. Fabbrichesi, R. Floreanini, and L. Marzola, About Witnessing Bell Non-locality at Colliders, *Found. Phys.* **55**, 83 (2025), arXiv:2503.18535 [quant-ph].

[56] M. Nielsen and I. Chuang, *Quantum Computation and Quantum Information*, Cambridge Series on Information and the Natural Sciences (Cambridge University Press, 2000).

[57] P. W. Shor, Polynomial time algorithms for prime factorization and discrete logarithms on a quantum computer, *SIAM J. Sci. Statist. Comput.* **26**, 1484 (1997), arXiv:quant-ph/9508027.

[58] P. W. Shor, Algorithms for quantum computation: discrete logarithms and factoring, in *Proceedings 35th Annual Symposium on Foundations of Computer Science* (1994) p. 124.

[59] L. K. Grover, A fast quantum mechanical algorithm for database search, in *Proceedings of the Twenty-Eighth Annual ACM Symposium on Theory of Computing*, STOC ’96 (1996) p. 212.

[60] L. K. Grover, Quantum mechanics helps in searching for a needle in a haystack, *Phys. Rev. Lett.* **79**, 325 (1997), arXiv:quant-ph/9706033.

[61] D. Gottesman, The Heisenberg representation of quantum computers, in *22nd International Colloquium on Group Theoretical Methods in Physics* (1998) p. 32, arXiv:quant-ph/9807006.

[62] K. Goto, T. Nosaka, and M. Nozaki, Probing chaos by magic monotones, *Phys. Rev. D* **106**, 126009 (2022), arXiv:2112.14593 [hep-th].

[63] L. Leone, S. F. E. Oliviero, Y. Zhou, and A. Hamma, Quantum Chaos is Quantum, *Quantum* **5**, 453 (2021), arXiv:2102.08406 [quant-ph].

[64] C. D. White, C. Cao, and B. Swingle, Conformal field theories are magical, *Phys. Rev. B* **103**, 075145 (2021), arXiv:2007.01303 [quant-ph].

[65] Z.-W. Liu and A. Winter, Many-Body Quantum Magic, *PRX Quantum* **3**, 020333 (2022), arXiv:2010.13817 [quant-ph].

[66] A. Gu, S. F. E. Oliviero, and L. Leone, Doped stabilizer states in many-body physics and where to find them, *Phys. Rev. A* **110**, 062427 (2024), arXiv:2403.14912 [quant-ph].

[67] S. F. E. Oliviero, L. Leone, and A. Hamma, Magic-state resource theory for the ground state of the transverse-field Ising model, *Phys. Rev. A* **106**, 042426 (2022), arXiv:2205.02247 [quant-ph].

[68] D. Rattacaso, L. Leone, S. F. E. Oliviero, and A. Hamma, Stabilizer entropy dynamics after a quantum quench, *Phys. Rev. A* **108**, 042407 (2023), arXiv:2304.13768 [quant-ph].

[69] P. S. Tarabunga, E. Tirrito, T. Chanda, and M. Dalmonte, Many-Body Magic Via Pauli-Markov Chains—From Criticality to Gauge Theories, *PRX*

Quantum **4**, 040317 (2023), arXiv:2305.18541 [quant-ph].

[70] S. Zhou, Z. Yang, A. Hamma, and C. Chamon, Single T gate in a Clifford circuit drives transition to universal entanglement spectrum statistics, *SciPost Phys.* **9**, 087 (2020).

[71] A. Gu, S. F. E. Oliviero, and L. Leone, Magic-Induced Computational Separation in Entanglement Theory, *PRX Quantum* **6**, 020324 (2025), arXiv:2403.19610 [quant-ph].

[72] S. Cepollaro, G. Chirco, G. Cuffaro, G. Esposito, and A. Hamma, Stabilizer entropy of quantum tetrahedra, *Phys. Rev. D* **109**, 126008 (2024), arXiv:2402.07843 [hep-th].

[73] L. Leone, S. F. E. Oliviero, and A. Hamma, Stabilizer Rényi Entropy, *Phys. Rev. Lett.* **128**, 050402 (2022), arXiv:2106.12587 [quant-ph].

[74] C. D. White and M. J. White, Magic states of top quarks, *Phys. Rev. D* **110**, 116016 (2024), arXiv:2406.07321 [hep-ph].

[75] P. Nason, A New method for combining NLO QCD with shower Monte Carlo algorithms, *JHEP* **11**, 040, arXiv:hep-ph/0409146.

[76] S. Frixione, P. Nason, and C. Oleari, Matching NLO QCD computations with Parton Shower simulations: the POWHEG method, *JHEP* **11**, 070, arXiv:0709.2092 [hep-ph].

[77] S. Frixione, P. Nason, and G. Ridolfi, A Positive-weight next-to-leading-order Monte Carlo for heavy flavour hadroproduction, *JHEP* **09**, 126, arXiv:0707.3088 [hep-ph].

[78] T. Sjöstrand, S. Ask, J. R. Christiansen, R. Corke, N. Desai, P. Ilten, S. Mrenna, S. Prestel, C. O. Rasmussen, and P. Z. Skands, An introduction to PYTHIA 8.2, *Comput. Phys. Commun.* **191**, 159 (2015), arXiv:1410.3012 [hep-ph].

[79] R. Aoude, E. Madge, F. Maltoni, and L. Mantani, Quantum SMEFT tomography: Top quark pair production at the LHC, *Phys. Rev. D* **106**, 055007 (2022), arXiv:2203.05619 [hep-ph].

[80] M. Fabbrichesi, R. Floreanini, and E. Gabrielli, Constraining new physics in entangled two-qubit systems: top-quark, tau-lepton and photon pairs, *Eur. Phys. J. C* **83**, 162 (2023), arXiv:2208.11723 [hep-ph].

[81] C. Severi and E. Vryonidou, Quantum entanglement and top spin correlations in SMEFT at higher orders, *JHEP* **1**, 148, arXiv:2210.09330 [hep-ph].

[82] F. Maltoni, C. Severi, S. Tentori, and E. Vryonidou, Quantum detection of new physics in top-quark pair production at the LHC, *JHEP* **3**, 099, arXiv:2401.08751 [hep-ph].

[83] R. Aoude, H. Banks, C. D. White, and M. J. White, Probing new physics in the top sector using quantum information, arXiv:2505.12522 [hep-ph] (2025).

## Appendix A: More results on discord

We present the measurements of the top antiquark discord,  $\mathcal{D}_{\bar{t}}$  and the difference in the discord of the top quark and antiquark,  $\mathcal{D}_t - \mathcal{D}_{\bar{t}}$  in Fig. 4.

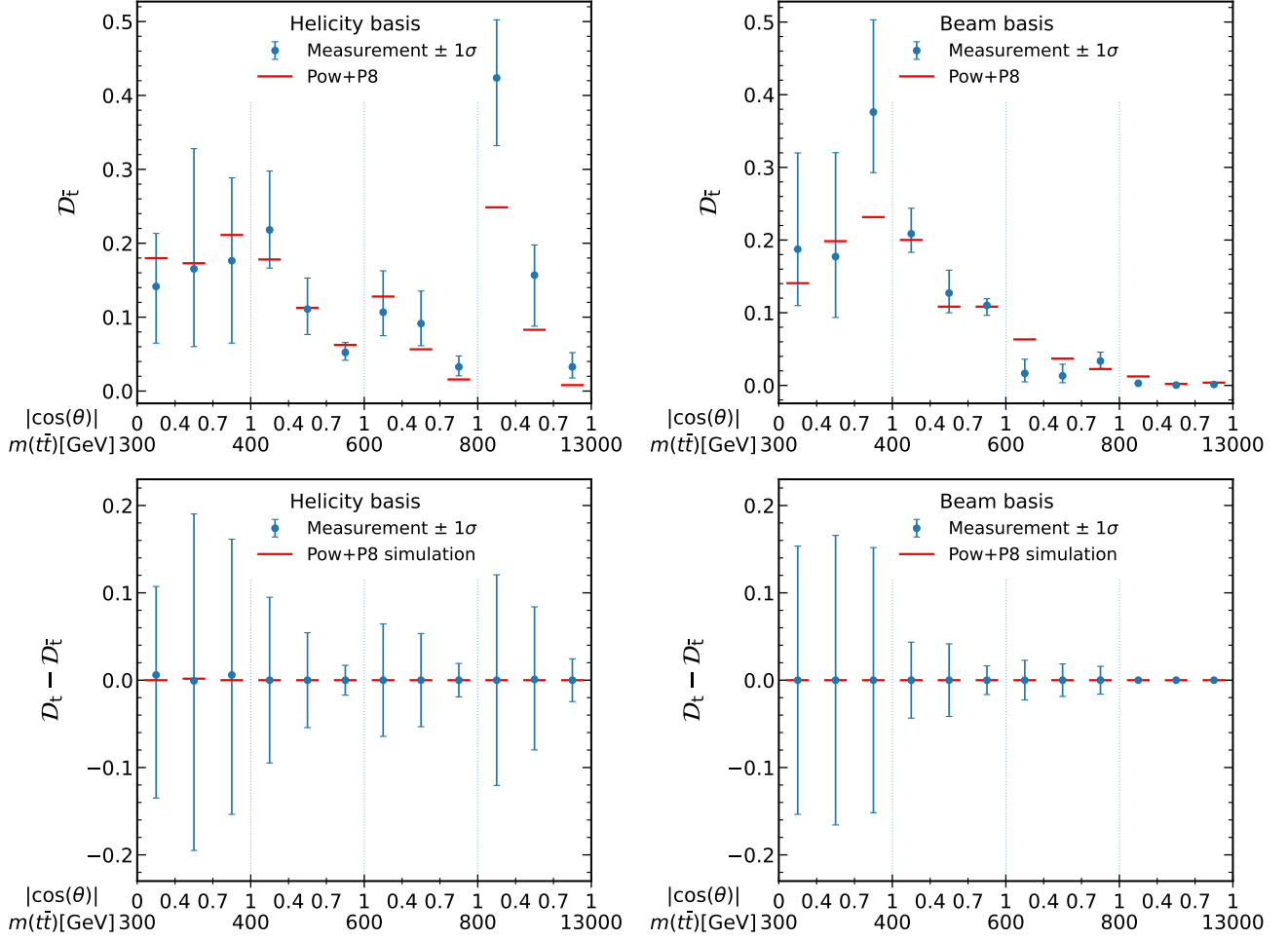


FIG. 4. Results of  $D_{\bar{t}}$  (upper row) and  $D_t - D_{\bar{t}}$  (bottom row) in bins of  $m(t\bar{t})$  vs.  $|cos(\theta)|$  in the helicity (left) and beam (right) basis. The measurements (points) are shown with the total uncertainty and compared to the predictions of POWHEG+PYTHIA. The threshold value for  $D_{\bar{t}}$  is zero.